photonics

MDPI

Article

Research on the Conversion Coefficient in Coherent Φ-OTDR and Its Intrinsic Impact on Localization Accuracy

Zhen Zhong [1,2,3,†], Ningmu Zou [3,4,*] and Xuping Zhang [3,*]

[1] School of Photoelectronic Engineering, Changzhou Institute of Technology, Changzhou 213032, China; zhongz@czust.edu.cn
[2] Jiangsu HNP Electric Technology Co., Ltd., Changzhou 213149, China
[3] Key Laboratory of Intelligent Optical Sensing and Manipulation, Ministry of Education, Nanjing University, Nanjing 210093, China
[4] Ingram School of Engineering, Texas State University, San Marcos, TX 78666, USA
* Correspondence: nzou@nju.edu.cn (N.Z.); xpzhang@nju.edu.cn (X.Z.)
† Affiliations 1 and 2 are co-first affiliations for joint and relative research topic, with no specified order.

Abstract: Phase-sensitive optical time domain reflectometry (Φ-OTDR) plays a crucial role in localizing and monitoring seismic waves, underwater structures, etc. Accurate localization of external perturbations along the fiber is essential for addressing these challenges effectively. The conversion coefficient, which links the detected phase signal to the perturbation signal on the fiber, has a significant impact on localization accuracy. This makes the characteristic of parameters relative to the conversion coefficient in Φ-OTDR a subject of deep research. Based on the coherent Φ-OTDR mathematical model, parameters like the modulus, the statistical phase, the phase change, and the peak difference are analyzed with and without the static region, respectively. When perturbations are homogeneously distributed along the fiber, the absence of static region on the phase change-fiber length plane leads to a nonlinear phase change relationship. This deviation from the expected linear relationship in the presence of static region means that the static region is essential for higher localization accuracy. The absence of static region results in a standard deviation of 0.042263 m for the localization deviation value, which could be theoretically reduced by a new sensor design with a static region. These findings underscore the importance of the conversion coefficient and the relevance of the static region in Φ-OTDR to achieving accurate and effective localization.

Keywords: conversion coefficient; static region; Φ-OTDR; localization accuracy

Citation: Zhong, Z.; Zou, N.; Zhang, X. Research on the Conversion Coefficient in Coherent Φ-OTDR and Its Intrinsic Impact on Localization Accuracy. *Photonics* **2024**, *11*, 901. https://doi.org/10.3390/photonics11100901

Received: 13 August 2024
Revised: 17 September 2024
Accepted: 23 September 2024
Published: 25 September 2024

1. Introduction

Fiber sensors integrated with optical grating, which are quasi-distributed, have played a great role in fields of seismic wave exploration [1], fiber-optic hydrophone [2], etc. However, the demodulation of fiber sensors integrated with optical grating is complicated and expensive. Recently, a distributed acoustic sensor (DAS) based on the principle of quantitative measurement of Φ-OTDR has been used to measure seismic waves and other vibration events [3,4]. Moreover, more and more researchers are focusing on how to achieve event localization and automatic tracking with the aid of Φ-OTDR [5,6]. Nevertheless, the impact of the conversion coefficient on the improvement of localization accuracy when the localization algorithm is based on the intensity of phase signal extracted by Φ-OTDR nearly has not been researched. Therefore, we first review the principle of Φ-OTDR.

As we know, for phase extraction in Φ-OTDR, the intensity trace which is directly proportional to the photocurrent is firstly acquired from the Φ-OTDR equipment (including the test fiber). Then, the phase value which contains the external perturbation information is extracted from these intensity traces. Many researchers have made great efforts on the process of phase extraction in Φ-OTDR [7–14]. According to the optical path difference concept, phase changes caused by external perturbations are proportional to the magnitude

of those perturbations. This relationship has been observed in numerous experiments focused on phase extraction in Φ-OTDR systems. However, previous studies on quantitative measurements with Φ-OTDR have mainly focused on phase differences between two points located before and after the perturbation region caused by external forces acting on a small section of the fiber. Correspondingly, in the process of calculation, we usually perform a differential operation for the phase values between two positions in the static region where the phase change or the other relative parameter along the fiber is not affected by any perturbation. However, in many cases such as seismic wave detection, the perturbation acts on all positions of fiber. In other words, there is no position without any perturbation. And the phase value of every position must be affected by the perturbation. Unfortunately, due to the bandwidth of the photodetector and the width of the optical pulse, the extracted phase of one position is the comprehensive result around this position. Then, the phase information extracted by the differential operation inevitably contains not only the phase difference between two positions but also the phase value induced by the perturbation around the two differential positions. That is to say, the calculated phase values based on the two positions have been affected by the action between the external perturbation and the fiber region around the two differential positions. Then, the conversion coefficient which is the ratio between the calculated phase signal and the physical perturbation signal may be changed for this reason. Since the characteristic of the phase change which is directly proportional to external perturbation signal in the direction of pulse sequence or peak difference which is proportional to the amplitude of the phase change can reflect this change in the conversion coefficient directly when a regular perturbation acts on the fiber homogeneously, we mostly and directly discuss the phase change or the peak difference in this paper for convenience. To the best of our knowledge, so far, there is no deep research on the characteristic of the conversion coefficient in Φ-OTDR, which is inevitable in many practical applications.

This study aims to investigate the characteristic of the conversion coefficient in Φ-OTDR in depth. To achieve this goal, the publicly known characteristic of the modulus which is the square root of Rayleigh backscattering light acting on the detector, the statistical phase which is the result of the inverse tangent operation, the phase change, and the peak difference in coherent Φ-OTDR with static regions were verified by simulating the mathematical model. Subsequently, through simulation and experiment, we researched the relative characteristic of coherent Φ-OTDR when it lacks static regions. Furthermore, by analyzing the simulation results of localization in a two-dimensional plane, we can gain insight into the effect of the undetermined conversion coefficient of coherent Φ-OTDR on the localization accuracy. Then, a potential solution of new laying structure of the test fiber is proposed to eliminate this intrinsic effect. Specifically, we can observe how the presence or absence of static regions affects the conversion coefficient and the subsequent localization accuracy. It is worth mentioning that noise in Φ-OTDR has been widely investigated in recent studies [15–18]. It is well known that noise can affect the localization accuracy. However, researchers have always ignored that the undetermined conversion coefficients of coherent Φ-OTDR itself also impacts the accuracy of localization. Further, it represents an intrinsic and essential influence that is more fundamental than the effects of noise. Overall, as far as we know, this study is the first to give a deeper understanding of the characteristic of the conversion coefficient in Φ-OTDR and its impact on localization accuracy. This study provides valuable insights that can be applied in the development of more accurate and reliable fiber-optic sensors for various applications.

2. Characteristic of the Conversion Coefficient

Figure 1 is a typical schematic diagram of traditional coherent Φ-OTDR. The highly coherent light from a laser device (LD) is divided into two branches via the 90:10 coupler. The upper branch light with 90% power is modulated by a pulse modulator (PM) to generate the probe pulse light whose width is from ns to us. Then, the probe pulse light is amplified by an erbium-doped optical fiber amplifier (EDFA) and injected into the test

fiber. The lower branch light with 10% power is used as the reference light. Rayleigh backscattering light from the test fiber and the reference light pass through a 50:50 coupler and enter a balanced photodetector (BPD). The detected signal by the BPD is sampled by an oscilloscope (OSC). When an external perturbation acts on the fiber, both the length of fiber and the fiber refractive index are changed. Except for the numerical difference, they have the same impact on the change in optical path difference or phase. For simplification in discussing the mathematical model of coherent Φ-OTDR, the change in fiber length is unified as the change in fiber refractive index in this article. When the noise factor and the coupling mode of detector are ignored, the Rayleigh backscattering light received by the balanced photodetector in coherent Φ-OTDR can be described as [19–21]:

$$E_B[z,t] = E_0 e^{-2\alpha z} \int_z^{z+\Delta z} \bar{r} q(x) \exp[j\frac{4\pi}{\lambda} \int_0^x n(y,t)dy]dx \quad (1)$$

where z is the distance from the input end of the fiber, Δz is relative to pulse width, t is the repetition time of the optical pulse, E_0 is the initial amplitude of Rayleigh backscattering light, α is the attenuation factor, $\bar{r}$ is the scattering factor which contains Rayleigh scattering coefficient, reverse capture coefficient and detection response rate, q is the waveform function of the optical pulse, λ is the wavelength of the optical pulse, and n is the fiber refractive index. It is noteworthy that for the phase response, the fiber refractive index n can be directly replaced by the differential refractive index Δn, which is obtained by subtracting the average refractive index along the fiber [20].

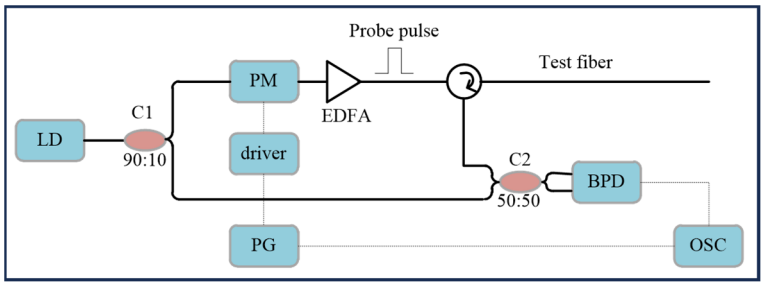

Figure 1. Schematic diagram of traditional coherent Φ-OTDR.

From Equation (1), the statistical phase can be directly obtained by the inverse tangent function and the result can be written as:

$$\Phi(z,t) = arc\tan\left\{\frac{\mathrm{Im}[E_B(z,t)]}{\mathrm{Re}[E_B(z,t)]}\right\} \pm k(z,t)\pi, k = 0,1,2\ldots \quad (2)$$

where *arc* tan is a symbol representing arctangent operation that takes into account the mathematical quadrant, k is determined by the phase unwrapping algorithm which is applied in the direction of pulse sequence for every sample position of the fiber, Im and Re denote imaginary and real parts of E_B, respectively.

For the arbitrary time t, $\Phi(z,t)$ is chaotic along the fiber for the inhomogeneous distribution of fiber refractive index and the randomness of the wrapped statistical phase. Therefore, $\Phi(z,t)$ cannot reflect the perturbation information well. In order to eliminate the irregularity of $\Phi(z,t)$ along the fiber, a reference phase $\Phi(z,t_0)$ is chosen where t_0 is the initial time of external perturbation acting on the fiber. Then, we can derive the phase change which is directly corresponding to the information of external perturbation by subtracting $\Phi(z,t_0)$ from $\Phi(z,t)$:

$$\varphi(z,t) = \Phi(z,t) - \Phi(z,t_0) \quad (3)$$

Although many researchers, including our team, have studied the amplitude and phase characteristics of Φ-OTDR in the static region, this paper uses the mathematical

model (Equations (1)–(3)) to demonstrate the consistent characteristics of Φ-OTDR, as previously validated in experiments. Conversely, the consistency between the simulation result and the experimental result would prove the validity of mathematical model. Then, we use this model to deduce the characteristic of Φ-OTDR without any static region. If an experimental result is consistent with the simulation result, it means the mathematical model is valid in Φ-OTDR without any static region. We believe that the research results based on the mathematical model will have a good guide for practical applications.

Due to the limit of computing capability, we set the pulse width as 1 *ns* when we simulate the amplitude and phase characteristic of coherent Φ-OTDR through Equations (1)–(3). Consequently, in the process of simulation, the length of test fiber in Figure 1 will be set relatively short. The constant E_0 in Equation (1) is assigned to be 1. The attenuation coefficient α is 0.2 dB/km. The variable $q(x)$ is a rectangular pulse and its amplitude is assigned to be 1. The wavelength λ is 1550 nm. The initial value $\Delta n(z, t_0)$ is a continuous uniform distribution in the range of $[-0.001, 0.001]$ on the whole fiber.

2.1. Coherent Φ-OTDR with the Static Region

Based on the mathematical model with the preset parameters, the characteristic of the modulus, the statistical phase, the phase change and the peak difference will be deeply analyzed for coherent Φ-OTDR with the static region. In order to induce the static region, a small region of test fiber in Figure 1 is acted by the external perturbation. Therefore, in the small set region [0.4426 m–0.4442 m] along the fiber with the whole length of 0.8 m, we add the variation δn, which denotes the vibration event and is described by:

$$\delta n(z, t) = 0.00005 * \sin(2\pi * 10^3 t) \tag{4}$$

Although the independent variable z is marked in $\delta n(z, t)$, δn does not change with z. Here, z only means that the set region [0.4426 m–0.4442 m] has a vibration event. Furthermore, we use $\Delta n(z, t) + \delta n(z, t)$ to replace $n(z, t)$ in Equation (1). For the convenience of calculation, the position of calculation for simulation is set at the back edge of the optical pulse and the simulation results are shown in Figure 2. In this figure, the last 0.2 m of the whole 0.8 m fiber is not displayed since it is impossible to calculate for lack of a full pulse.

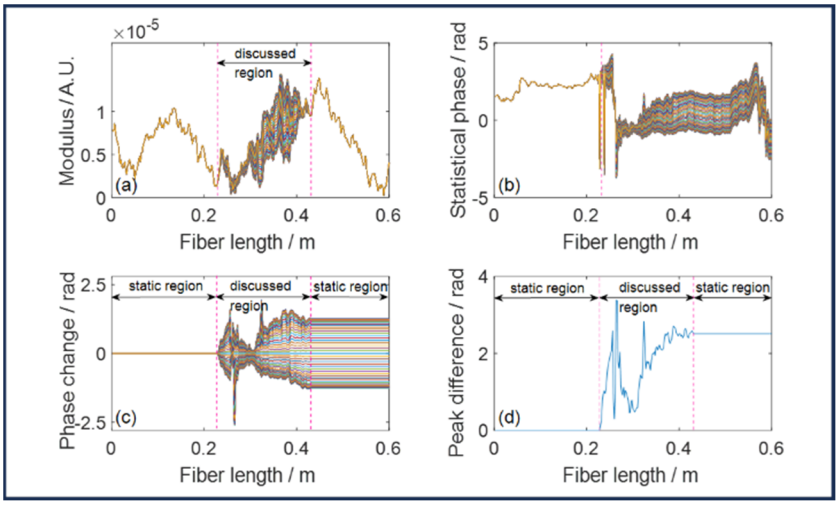

Figure 2. Simulation result in coherent Φ-OTDR with the static region (**a**), the modulus (**b**), the statistical phase (**c**), the phase change and (**d**) the peak difference.

In Figure 2a–c, every horizontal coordinate value corresponds to 80 vertical coordinate values from 80 pulses. Figure 2a is the superposition of 80 consecutive OTDR traces which are the modulus of Equation (1) (adding the action of Equation (4)). One OTDR trace corresponds to one pulse. In the practical application, the detected OTDR trace in coherent

Φ-OTDR contains the intermediate frequency part induced by the pulse modulator which has a frequency shift and appears more complex than the trace in Figure 2a. However, if the detected OTDR trace in coherent Φ-OTDR eliminates the intermediate frequency part and the proportional coefficient is ignored, the remaining part is just the modulus-based OTDR trace in Figure 2a. In region [0.2426 m–0.4442 m], we can see that the modulus at one position of fiber has many values. However, the modulus in the position of other regions seems have only one value. Ignoring the effect of pulse width, we can judge the position of the vibration acting on the optical fiber by this difference. Carefully comparing the set region [0.4426 m–0.4442 m] with the discussed region [0.2426 m–0.4442 m] in Figure 2a, we can find that the discussed region is nearly 0.2 m more than the set region. This is because the pulse width is 0.2 m (1 ns) which is bigger than the length of set region. And the process of action between the vibration and the optical pulse begins when the front edge of the optical pulse encounters the vibration event and ends when the back edge of the optical pulse leaves the vibration event.

In Figure 2b, the superposition result of the calculated statistical phase according to Equation (2) is shown. In this subfigure, the statistical phase of one position begins to have many different values at 0.2426 m (the substantial variation in values of the statistical phase right before 0.2426 m is generated by phase jumps during the phase unwrapping process. In fact, there is only one phase value at each position before 0.2426 m), and it continues until the end of the optical fiber. This is the biggest difference between Figure 2a,b. In other words, only from the image of the statistical phase in Figure 2b, the beginning of the vibration region can be easily estimated. But it is difficult to determine the end of the vibration region. Therefore, the vibration region cannot be discriminated by the statistical phase in Figure 2b. Moreover, the irregularity of the statistical phase along the whole fiber has been obviously shown in this subfigure. This is mainly induced by the random fiber refractive index and the scattering factor. Thus, the statistical phase is difficult to accurately represent the information of external perturbation on the fiber.

In order to acquire the accurate phase signal which is not affected by the random initial phase (wrapped statistical phase) along the fiber, we further deal with the data in Figure 2b according to Equation (3). Then, the calculated phase change shown in Figure 2c is obtained. The phase change in the position of fiber less than 0.2426 m is zero. That is because there is no perturbation acting on the initial region. So the initial region is the static region. In the discussed region [0.2426 m–0.4442 m], the phase changes in all positions are chaotic for the inhomogeneous distribution of the fiber refractive index, the effect of perturbation signal and the interference fading. However, in the remaining region, the phase change seems to be a straight line on the phase change-fiber length plane. The remaining region is also the static region. And these straight lines whose slopes are zero mean that the information of external perturbation could be represented by the waveform of the phase change at any position right behind the discussed region.

To better demonstrate the linear characteristic of the phase change in the static region of coherent Φ-OTDR, based on the data in Figure 2c, we perform the differential operation between the maximum and minimum values of the phase change at every position of the fiber. Then, one position has a peak difference and all values of the peak difference along the fiber are plotted in Figure 2d. In this subfigure, the linear line in the static region can be easily observed. Because the value of the peak difference is proportional to the amplitude of the external vibration event, the peak difference can directly reflect the characteristic of the conversion coefficient.

In addition, according to the traditional method of acquiring the spatial resolution, we perform the differential operation between OTDR traces in Figure 2a. Then, the differential value is shown in Figure 3a. In this figure, we can find that FWHM is about 0.1 m. Since the simulation model of Φ-OTDR is ideal, the FWHM value at this point should represent the limit of spatial resolution (or named spatial resolution limit). This means that the spatial resolution limit derived from the simulation data is just half the pulse width, which is consist with the traditional cognition. Furthermore, we perform more research on the

quantitative relationship of measurement in coherent Φ-OTDR. In simulation, the vibration event added is also in the form described by Equation (4). But the vibration amplitude which is proportional to the amplitude of $\delta n(z,t)$, the vibration length which is the distance of small region of fiber acted by the external vibration, the position of the vibration may be changed according to the requirement of research. Then, defining the final peak difference as the value of the peak difference at the position of 0.6 m, the simulation results are obtained and shown in Figure 3b, 3c and 3d, respectively. By fitting the simulation data final peak difference—vibration amplitude in Figure 3b and the simulation data final peak difference—vibration length in Figure 3c, the standard deviations of linear fitting are 2.23 × 10^{-10} rad and 1.3 × 10^{-15} rad, respectively. The low standard deviation values mean that the final peak difference is linearly with the vibration amplitude/vibration length. Then, we can deduce that when a coherent Φ-OTDR is used to measure the external perturbation at one position, the SNR of the measured signal can be improved by twisting the fiber repeatedly. In addition, we find that although the position of the vibration is different, the final peak difference nearly has no change. This means that the measured result in coherent Φ-OTDR has nothing to do with the position. It is worth noting that the linewidth of laser in the optical fiber may be changed when Rayleigh backscattering light propagates along the fiber. Then, it may slightly affect the result of quantitative measurement. Fortunately, the linewidth of laser used in Φ-OTDR is ultra-narrow and it will be slightly narrowed with the propagation of signal light. Consequently, the change in linewidth in the practical application can be ignored. Therefore, if the quantitative relation at any position of the optical fiber in coherent Φ-OTDR with the static region is calibrated, this quantitative relation can be applied to other position of fiber.

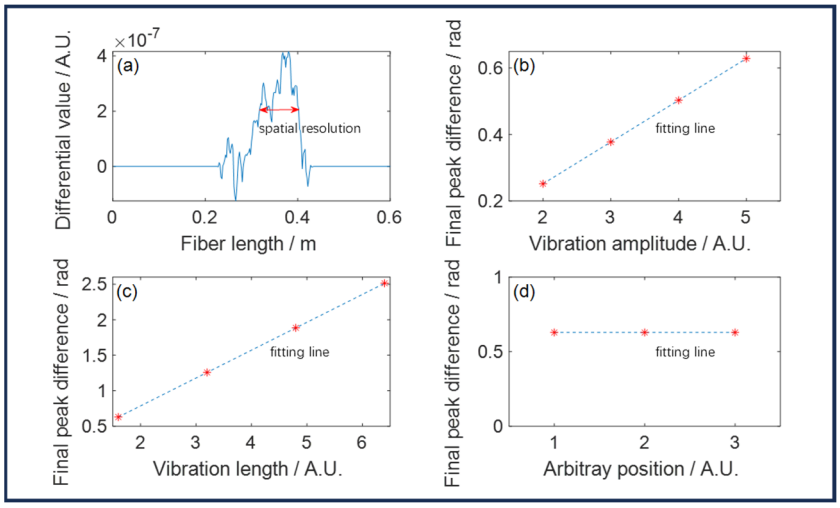

Figure 3. (**a**) Differential value for spatial resolution; relationship between final peak difference and (**b**) vibration amplitude/(**c**) vibration length/(**d**) position of the fiber.

2.2. Coherent Φ-OTDR without the Static Region

In Section 2.1, the characteristic of coherent Φ-OTDR with the static region has been researched. The simulation results are consistent with what was expected in the experiment. Based on this, we use this mathematical model to analyze the characteristic of coherent Φ-OTDR without any static regions. Assuming all region of test fiber in Figure 1 is acted by the same vibration event, we add the variation $\delta n'$ depicted in Equation (5) in all region of fiber:

$$\delta n'(z,t) = 0.0000005 * \sin(2\pi * 10^3 t) \quad (5)$$

Here, every position of z has the same $\delta n'$. Then, we also use $\Delta n(z,t) + \delta n'(z,t)$ to substitute $n(z,t)$ in Equation (1). Since the amplitude of the vibration acted on all positions of fiber is the same, the characteristic of the phase change/peak difference for this

simulation result can directly reflect the characteristic of the conversion coefficient. With the action of Equation (5), the simulation results are shown in Figure 4.

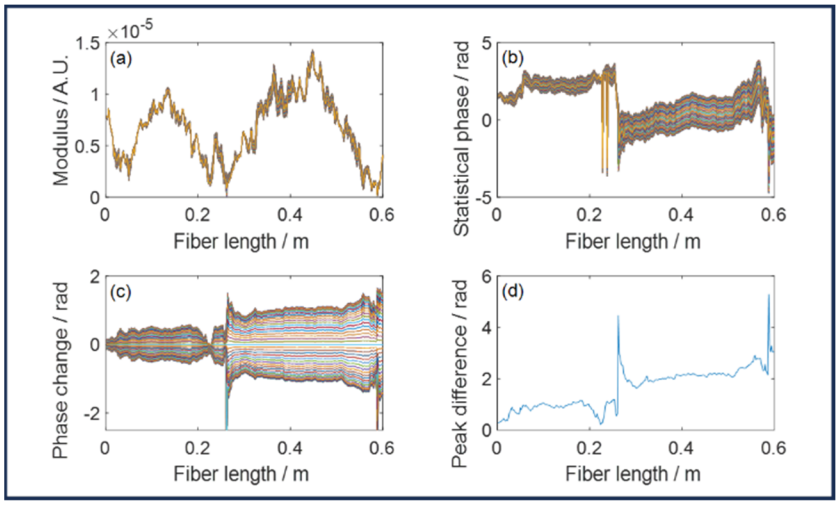

Figure 4. (**a**) The modulus, (**b**) the statistical phase, (**c**) the phase change and (**d**) the peak difference when the external perturbation acts equally on every position of the fiber.

Figure 4a is the superposition of 80 consecutive OTDR traces when every position of the fiber is acted by the same perturbation. One OTDR trace (usually corresponding to one color in the figure) is also relative to one pulse. In Figure 2a, some positions have many modulus values while other positions have only one modulus value. In contrast, In Figure 4a, the OTDR trace at every position has many different values. This means that the OTDR trace varies with the pulse sequence at every position. By this varying characteristic in Figure 4a, we can judge that every position of the fiber is affected by the external perturbation that is consistent with what we expected.

Similar to the investigation of traditional coherent Φ-OTDR with the static region, this study focuses on analyzing the parameters associated with the conversion coefficient when Φ-OTDR lacks a static region. Subsequently, the statistical phase is obtained from the data presented in Figure 4a and is plotted in Figure 4b. It can be observed from this subfigure that the statistical phase range at a given position increases with the fiber length, although it distributes irregularly throughout the fiber. When traditional coherent Φ-OTDR has a static region, the statistical phase in Figure 2b is converted into the phase change in Figure 2c to establish the regularity of phase characteristic. Similarly, Figure 4b is transformed into Figure 4c to acquire the phase change. Unfortunately, no linear distribution of the phase change along the fiber is evident in Figure 4c, despite the observable increase in the phase change range at a given position with the fiber length.

To better demonstrate the relationship between the phase change and the fiber length, we also calculate the peak difference according to the data in Figure 4c and the differential result is depicted in Figure 4d. Obviously, there is still no linear characteristic in this subfigure.

The magnitude of the vibration applied to the fiber is consistent at every position of the fiber. And, in coherent Φ-OTDR, the phase information of subsequent position contains the phase information of foregoing position. Therefore, we guessed that the phase change in Figure 4c and the peak difference in Figure 4d should increase linearly with the increase in fiber length. However, as has been demonstrated in these two subfigures, we cannot find any linear profile along the fiber. In the practical application, we usually perform a differential operation between two positions for retrieving the phase information of one perturbation. As shown in Figure 4c, if the fiber is divided into equal bands and the differential calculation is applied to the phase changes at the ends of each band, we would expect to obtain consistent results for the same perturbation across all bands. However,

although we can see the sine waveform which is not displayed here, we cannot obtain equal results for different differential results at these bands. In a word, we cannot obtain the same phase signal for the different bands although every band has the same perturbation. Thus, we can further deduce that the loss of linear characteristic of the phase change/peak difference along the fiber in coherent Φ-OTDR means the loss of the capability of having the accurate conversion coefficient between the retrieved phase signal and the perturbation source when coherent Φ-OTDR is applied for quantitative measurement with the full perturbation on the fiber. Because the conversion coefficient at the different positions of fiber is not accurate at this point, we can guess that the localization accuracy of perturbation signal may not be accurate.

As has been discussed above, the parameter relative to the conversion coefficient in coherent Φ-OTDR without the static region is nonlinear with its dependent variable. In order to further illustrate this phenomenon, we directly plot the simulated phase changes at the positions of 0.2 m, 0.4 m and 0.6 m in Figure 5a. The amplitudes of three traces are 0.45 rad, 1.08 rad, and 1.51 rad, respectively. At this point, the differential values between amplitudes of two end for one 0.2 m band are 0.63 rad and 0.43 rad. The two unequal numerical values mean that the conversion coefficient is not constant. In coherent Φ-OTDR with the static region, the constant conversion coefficient or relative characteristic has been observed in many experiments. However, to best of our knowledge, the is no experimental result about the characteristic of parameters relative to the conversion coefficient at the different position of the fiber in coherent Φ-OTDR without the static region. To demonstrate the correctness of the simulation results in Section 2.2 to a certain extent, a simple experiment is performed. Except for a PZT wrapped by 60 m fiber at the position of about 3 km, the experimental setup is consistent with what is described in Figure 1. The laser device LD is NKT E15 which has a high stable frequency and high coherent laser. The light from E15 is modulated by an acousto-optic modulator into a 100 ns probe pulse light. The pulse width and the spatial resolution limit are 20 m and 10 m, respective. Both values are much smaller than 60 m which is the length of region acted by PZT. Consequently, the phenomenon in and near the 60 m fiber region can be considered as the characteristic in coherent Φ-OTDR with full region of perturbation. When a 1 V sinusoidal voltage acts on PZT, if the accuracy of coordinate starting point is ignored, the phase change in Figure 5b is obtained. The phase change in region [1000 m, 1060 m] acted by PZT is zoomed and redrawn in Figure 5c. Except the noise, the phase change varies slowly before and behind this region. So the rest region is not displayed in Figure 5c. From Figure 5c, we can find that the amplitude of the phase change in Figure 5c increases totally with the fiber length, which is similar with that in Figure 4c. And we also can find that the phase change is indeed nonlinear with the fiber length. Further, we plot phase changes at the positions of 1030 m, 1046 m and 1052.8 m in Figure 5d. Correspondingly, trace A, trace B and trace C have been shown. Due to the fact that these three traces are derived from experimental data, they may be subject to the influence of noise. Since the experiment utilized a laser with extremely low frequency drift, the phase calculated from the experimental data is mainly affected by the residual noise within the passband of the low-pass filter used in the quadrature demodulation. To mitigate this effect, we fitted trace A, trace B, and trace C with parameterized sine curves, obtaining approximate true values for the amplitudes of 27.76 rad, 46 rad, and 57.42 rad, respectively. This results in the three data points (1030, 27.76), (1046, 46), and (1052.8, 57.42). Obviously, these three data points do not lie on a straight line. The vertical distance between point (1046, 46) and the straight line formed by points (1030, 27.76) and (1052.8, 57.42) is 2.864 rad, which is significantly larger than the noise floor of phase changes induced by the residual noise after filtering. Therefore, it can be inferred that the nonlinear alignment of the points (1030, 27.76), (1046, 46), and (1052.8, 57.42) is not decided by noise, but rather by the inconsistency of the conversion coefficient. In a word, the experimental results show that the conversion coefficient in coherent Φ-OTDR without the static region is not constant, which is consistent with what was found by the simulation results.

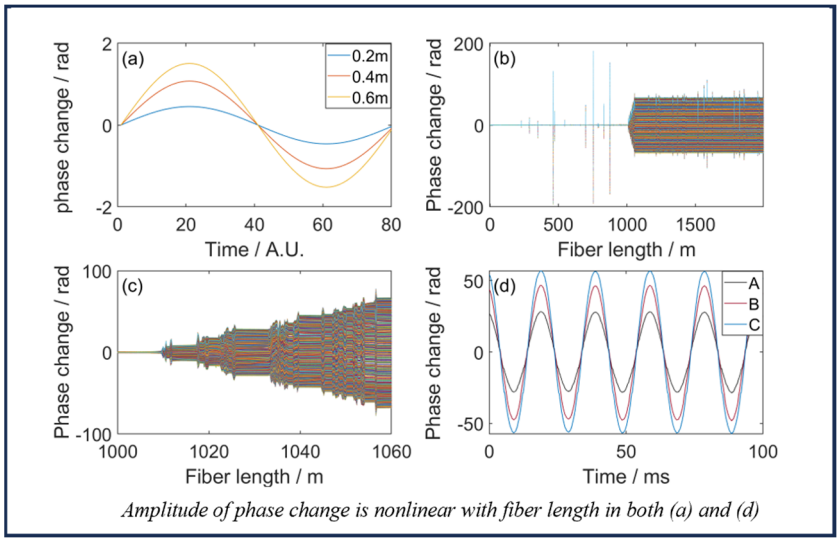

Figure 5. Simulation results: (**a**) the phase change at three different positions; experimental results: (**b**) the phase change, (**c**) the local magnification of (**b**), and (**d**) the phase change at three different positions.

3. Intrinsic Impact of the Conversion Coefficient on Localization Accuracy

In the last section, the characteristic of parameters related to the conversion coefficient of coherent Φ-OTDR under two different types of vibration events is described in detail. For the first type of vibration event which is acting on the small region of fiber, the phase change/peak difference has the static region. At this time, we can consider that the traditional Φ-OTDR without any special design has a constant conversion coefficient and it can afford an accurate measurement. Conversely, when the entire fiber is subjected to the second type of vibration event, there is no static region on the phase change/peak difference-fiber length plane. At this point, the traditional Φ-OTDR without any special design has an undetermined conversion coefficient which varies with the position of fiber. Then, it is difficult to acquire an accurate measurement result. Unfortunately, the perturbation sources in many practical applications are similar to the second type of vibration event. For example, a fiber-optic hydrophone is used to detect the enemy target. If the fiber is not specially processed, the acoustic signal from the enemy target acts on the whole fiber. Consequently, in this section, we firstly analyze the impact of the undetermined conversion coefficient on the accuracy of localization. Then, we give a potential solution of eliminating the impact of the undetermined conversion coefficient.

3.1. Impact of the Undetermined Conversion Coefficient

Here, we do not consider the influence of noise on localization accuracy. Then, the error of localization induced by the traditional Φ-OTDR without any special design is inherent. As has been shown in Section 2, the peak difference can reflect the characteristic of the conversion coefficient. Consequently, we directly use the value of the peak difference to research the capability of localization by the traditional coherent Φ-OTDR. In order to speed up the calculation, we slightly reduce the number of particles per unit in one pulse. Then, a plot of the peak difference when the perturbation acts uniformly on the whole fiber in Figure 1 is obtained and shown in Figure 6a. Because the peak difference in this subfigure is not linear with the fiber length, the conversion coefficient must be undetermined at different positions of fiber. For purpose of simplicity, we normalize peak difference values at the positions of 0.6 m, 1.2 m, and 1.8 m at the horizontal axis and the denominator of normalization is determined by the coordinate values and the benchmark together. Then, the localization result is calculated based on the traditional coherent Φ-OTDR (in Figure 1) in which there is no static region. During the calculation process, we make the assumption that the acoustic signal, which is the source of perturbation, acting

on the fiber is a scalar quantity. At the same time, we assume that the acoustic signal is arranged in a two-dimensional plane with a horizontal axis and a vertical axis. The value of each axis is from 0 m to 1.8 m. So a 1.8 m long fiber is placed along the horizontal axis and this axis is just "fiber length" in Figure 6a. For the convenience of the display, the vertical axis is defined as "vertical length" and there is no fiber on this axis. Then, the process of localization is based on this two-dimensional space and an acoustic signal simulated by a vibration event is fixed at the position of (1.2 m, 1.2 m).

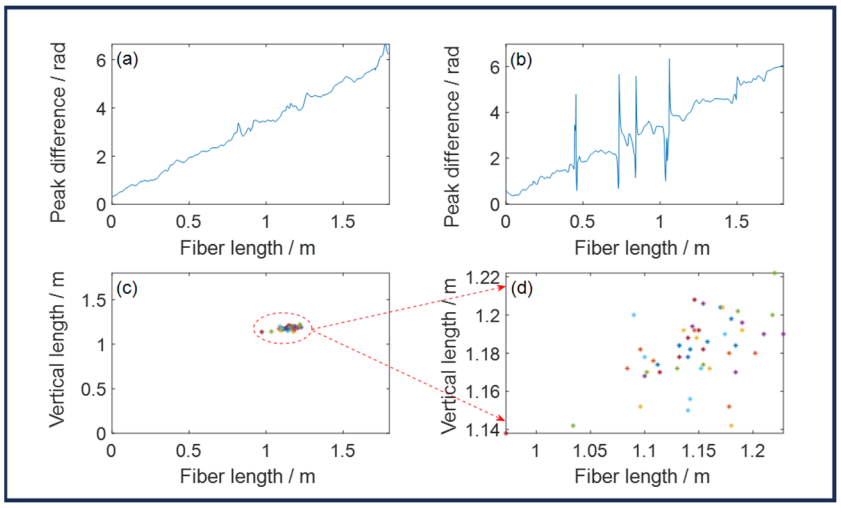

Figure 6. (**a**) One peak difference-fiber length plot when the perturbation acts on all positions of fiber in traditional coherent Φ-OTDR; (**b**) localization results for 50 different peak difference-fiber length plots.

The calculation process of localization is described in detail as follows:

Step 1: Ignoring the effect of noise, to acquire the peak difference values which can directly reflect the effect of the conversion coefficient in Figure 6a;

Step 2: Three peak difference values at the positions of (0.6 m, 0 m), (1.2 m, 0 m), and (1.8 m, 0 m) (in practical applications, the coordinate values of these three positions need to be calibrated with a comprehensive consideration of spatial resolution in a one-dimensional line and the signal-to-noise ratio of detected signal) are converted into normalized values;

Step 3: Dividing the plane (1.8 m × 1.8 m) into several units in 0.002 m × 0.002 m which is limited by the computational capability and the minimum sampling interval along the fiber;

Step 4: Assuming every vertex of each unit is the position of acoustic signal, to calculate the sum of error based on three normalized values for each vertex;

Step 5: To find the position of vertex where the sum of error is minimum. And we consider it as the extracted position of acoustic signal.

After a series of calculations, we obtain that the extracted position of acoustic signal is (1.17 m, 1.204 m). Although it is close to the expected position (1.2 m, 1.2 m), an error caused by the intrinsic characteristic of the undetermined peak difference/conversion coefficients reflected in Figure 6a indeed emerges. Since the test fiber is part of the Φ-OTDR system, and the inconsistency of the conversion coefficient at various positions along the fiber is an inherent characteristic of the coherent Φ-OTDR system without any static region. Therefore, testing with a different fiber can help to investigate the impact of the undetermined conversion coefficient on localization error. Switching to a new fiber implies a new refractive index distribution and a new profile of the conversion coefficient. Figure 6b just reflects the new distribution of the conversion coefficient along the fiber. Since the new peak difference-fiber length plot in Figure 6b is obviously different from that in Figure 6a, it will most likely yield a new localization result. Furthermore, the localization process based on the different test fiber is totally performed 50 times, and all the localization results are

drawn in Figure 6c. From this subfigure and Figure 6d (zoomed-in detail of Figure 6c), we can find that the maximum and the minimum distances deviated from the perturbation source are 0.23628 m and 0.01077 m, respectively. At the same time, we can acquire that the standard deviation of deviation values is 0.042263 m which is 2.1 times as large as the grid unit value 0.02 m. This indicates that the undetermined conversion coefficient introduces an error into the localization process of traditional coherent Φ-OTDR.

3.2. Potential Solution with Designed Static Region

For different conversion coefficient values at the different positions of fiber in the traditional Φ-OTDR without any special design, the phase signal of perturbation cannot be accurately measured. At this point, it will result in an error of localization. However, in many practical applications such as fiber-optic hydrophone, the perturbation is acting at every position of the fiber if the laying of fiber structure has no special processing. At this time, the fiber-optic hydrophone constructed by the traditional Φ-OTDR without any special design will lose the capability of accurate measurement. Sometimes, the method of fiber embedded with FBG is used to obtain the accurate measurement result. In this method, the change in strain induced by the external perturbation is investigated by observing the change in optical spectrum. So the signal demodulation in the scheme of the fiber sensor with FBG is more complex. Consequently, a new scheme of a fiber sensor which can avoid the complicated demodulation process in the FBG based instrument and can obtain the accurate measurement result will be welcomed.

Based on the fact that coherent Φ-OTDR with the linear characteristic of the phase change/peak difference along the fiber means the constant conversion coefficient at different positions in the static region, in this article we perform a special processing for the laying of fiber structure of traditional coherent Φ-OTDR in Figure 1. Then, we obtain a new fiber sensor with a distribution of fiber rings and shield regions as shown in Figure 7. In the new fiber senor, there is no FBG and the process of signal demodulation does not involve the change in optical spectrum, so the demodulation process is relatively easy.

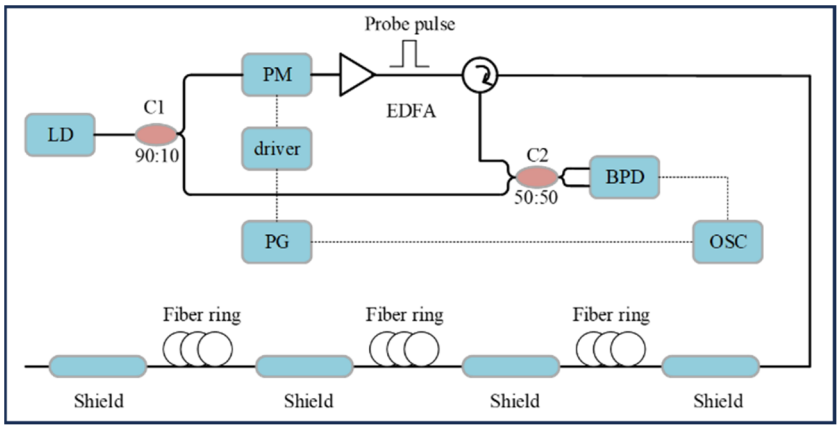

Figure 7. Scheme of a new fiber sensor using coherent Φ-OTDR with shield regions of fiber and fiber rings.

Except for the fiber part, all devices in Figure 7 are the same as those in Figure 1. Therefore, the new fiber sensor can be easily and digitally demodulated by IQ demodulation which is used for the phase extraction in the traditional coherent Φ-OTDR without any special processing. At the same distance in Figure 7, one part of fiber is shielded. The shield region is usually bigger than two times pulse width. This may decrease the traditional spatial resolution which affects the localization accuracy. This is because, if the new sensor is applied to one-dimensional application, the shield regions containing static regions cannot sense the external perturbation signal. At this point, it limits the precision of event localization. However, it can be easily compensated by the laying structure of optical

fiber. Further, if Φ-OTDR in Figure 7 is used for acoustic localization in a two-dimensional space, the positional coordinate for each point on the fiber is clear. In the shield region, no perturbation can act on this part of fiber. A comparison of Figures 2a–d and 4a–d shows that the shied region could provide the emergence of the linear phase change/peak difference even if the external perturbation acts on all regions (except for the shied region) of fiber, which guarantees a determined and constant conversion coefficient value. It is worth noting that the static region in the new fiber sensor is in the shield region, but the length of the static region is smaller than that of the shield region. Between two adjacent shield regions, there is a fiber ring that is twisted by the fiber itself. Although the fiber ring has a large number of turns, it fixes at one position of the fiber. And the diameter of fiber ring is usually in the order of decimeter. Therefore, compared the space of fiber ring with the length of whole fiber in the practical application, the fiber ring in space can be regarded as a point in a long line. Then, each loop of the fiber ring can be considered to have the same response to one perturbation. Moreover, according to the relationship demonstrated in Figure 3c, the greater the loop number of fiber rings, the greater the amplitude of phase signal. Correspondingly, the SNR of phase signal retrieved by differential operation between two positions in the adjacent shield regions can be expressed as

$$SNR = N \cdot \frac{A_{signal}}{A_{noise}} \tag{6}$$

where N is the loop number of fiber ring, A_{signal} is the amplitude of phase signal for a single loop, and A_{noise} is the amplitude of the phase change noise in coherent Φ-OTDR. For differential operation between two positions, A_{noise} almost does not change even if the loop number of fiber ring changes. As has been discussed in Section 2.1, all the fiber rings at different positions in the static region on the phase change-fiber length plane have accurate conversion coefficient values and have the same capability of accurate measurement. Consequently, the SNR of a new fiber sensor can be easily improved by increasing the loop number of fiber rings.

Obviously, if we use the new fiber sensor in Figure 7 to localize the acoustic signal, there are static regions and the conversion coefficient is constant. Since the influence of noise and the grid unit described in Section 3.1 is still ignored, all conditions are ideal. Therefore, regardless of which calculation method is used to obtain the localization results, the final extracted position based on the new fiber senor must be what we expected. At this point, the error induced by the calculation is at most 0.028 m due to the grid unit value being 0.02 m. In other words, if the localization error is exclusively a result of the uncertainty in the conversion coefficient and the effect of the minimum grid unit in the computational method, the error from using the new proposed fiber sensor in Figure 7 is no more than 67% of the error produced by a traditional Φ-OTDR without any special design. Consequently, if the localization executed by Φ-OTDR needs a higher accuracy, the scheme of a new fiber sensor which is described in Figure 7 is a good choice.

4. Discussion

In our mathematical model, the noise has not been considered. That is why the calculated standard deviation in Section 2.1 is lower than the noise level in the practical application. For the Φ-OTDR in use, there are noises such as polarization noise [22], interference noise, the noise of reference light, and thermal noise of detector. All these noises enter the photocurrent of detector. When the phase value is demodulated from the detected OTDR trace which is linearly transformed from the photocurrent, these noises exhibit in the form of the phase. Worse still, the phase signal is completely lost when polarization noise predominantly appears. This is because the polarization noise severely distorts the waveform of phase signal in the position of polarization fading. For other noises, they may slightly decrease the SNR of phase signal. But the waveform of phase signal still can be found. Therefore, the effect of polarization noise should be firstly eliminated in coherent Φ-OTDR. The phase changes in the static region (except for positions of the

phase change noise) are linear with the fiber length. And the final phase signal can be accurately retrieved based on two linear regions. At this point, the polarization fading in the static region can be easily discriminated by the linear characteristic of the phase change. In addition, noises are not considered in the comparison of localization accuracy of different schemes in Section 3.2. On the one hand, all results are based on the inherent characteristic of different schemes. On the other hand, the localization resolution may be decreased if noises are added in the process of simulation. Therefore, in the practical application, the improvement of localization resolution will be jointly decided by inherent characteristic of localization method, noise and other factors. It is important to note that in practical application systems, we always aim to enhance the signal-to-noise ratio (SNR) to improve the accuracy of localization. However, when the SNR is increased to a certain level (which corresponds to a certain degree of localization accuracy), if the effect of undetermined conversion coefficients is not mitigated, the localization accuracy calculated from actual measurement data will not be further improved (even if the grid on the two-dimensional plane in the localization algorithm is infinitely small). Therefore, eliminating the influence of undetermined conversion coefficients is a fundamental prerequisite to achieving precise localization.

In our simulation in Section 2, the pulse width is only 1 ns for the limit of computing capability. But in the present, the pulse width of Φ-OTDR in the practical application is usually more than 10 ns. However, the simulation result with the pulse width of 1 *ns* is meaningful. On the one hand, with the advancement of technology, the device applied for Φ-OTDR with the pulse width of 1 ns will be easily gotten. At this point, Φ-OTDR can be applied in small-scale applications such as health monitoring of the human body. On the other hand, a numerical value obtained in a simulation comes from the calculation of 1,129,000 particles. The size of this number is large enough that the statistical features of the simulation results will not be altered by the presence of a larger number of particles. Consequently, the simulation results under the condition of 1 ns have a positive reference significance for Φ-OTDR with a pulse width of 10 ns or more in practical applications.

Here, we give a qualitative analysis of the differences in conversion coefficients between Φ-OTDR systems with and without static regions. According to [20], Equation (1) corresponds to the detection result at a certain fiber sampling position by the detector. This is related not only to the pulse width, which corresponds to N scattering particles, but also to the detector's response period (or the data acquisition time slot), which corresponds to M scattering particles. Further, N is much larger than M. The phase factor in the exponential term on the right side of Equation (1) is relative to the cumulative phase value along the light path up to that certain fiber sampling position, with a cumulative length of at least one pulse width. Since the value of N is large, the cumulative effect of the phase factor appears uniform despite the inhomogeneous distribution of the fiber refractive index. This is why, in a coherent Φ-OTDR with static regions, the amplitude of the phase signal is directly proportional to the length of the perturbed region. The term $\bar{r}$ in Equation (1) is related to the phase value, which is the phase difference between pairs of scattering particles among the M particles. Since M is a smaller value, the result of the summation does not exhibit uniformity, meaning that the value of $\bar{r}$ is different at different fiber sampling positions. This is why the statistical phase in non-perturbed regions does not show a regular sawtooth pattern in the direction of fiber length. Since the phase value in $\bar{r}$ is the phase difference between pairs of scattering particles, the value of $\bar{r}$ is the same between different pulses, regardless of whether there is a perturbed region before the static region. This leads to a linear distribution of phase changes along the fiber in the static region. Then, by taking the differential operation in the static regions on either side of the perturbed region to solve for the phase signal, the influence of $\bar{r}$ is naturally eliminated, and the solved phase signal is independent of the position of the perturbation on the fiber but is related only to the length and the intensity of the perturbation. The effect of length acted by the perturbation has already been discussed. Regarding the intensity, the stronger the perturbation, the greater the degree of change in the fiber refractive index, and consequently, the greater

the change in the phase. Additionally, the influence of $\bar{r}$ on the conversion coefficient of coherent Φ-OTDR aids in understanding the precise solution of phase signals in Φ-OTDR based on direct detection.

5. Conclusions

In this article, based on the established mathematical model for quantitative measurement of coherent Φ-OTDR, the parameters relative to the conversion coefficient when coherent Φ-OTDR has the static region and has no static region are deeply studied, respectively. Furthermore, when coherent Φ-OTDR has the static region, the linear relationship between the peak difference and the amplitude/length of vibration acting on the fiber is verified. It is also revealed that the peak difference does not change with the change in position of the fiber. However, the research result in coherent Φ-OTDR without the static region shows that the retrieved phase change cannot accurately and quantitatively reflect the amplitude of external perturbation. Therefore, to achieve accurate localization results, the presence of a static region in coherent Φ-OTDR systems is crucial. Based on the necessity of having the static region and enhancing the SNR of phase signal, a scheme of a new fiber sensor with the shield regions of fiber and fiber rings has been proposed for accurate localization. With the aid of the newly proposed method, the error of localization in the traditional coherent Φ-OTDR can be theoretically and significantly reduced. In the future, we will focus on the development of fiber with shielded regions and will apply the new sensor to real-world scenarios.

Author Contributions: Conceptualization, Z.Z. and X.Z.; methodology, Z.Z. and N.Z.; software, Z.Z.; validation, Z.Z., N.Z. and X.Z.; formal analysis, N.Z.; investigation, Z.Z.; resources, X.Z.; data curation, Z.Z. and N.Z.; writing—original draft preparation, Z.Z.; writing—review and editing, N.Z.; visualization, Z.Z.; supervision, X.Z.; project administration, X.Z.; funding acquisition, X.Z. and Z.Z. All authors have read and agreed to the published version of the manuscript.

Funding: This research was funded by National Natural Science Foundation of China, grant number 61627816 and 62175100; Fundamental Research Funds for the Central Universities, grant number 021314380211; Jiangsu Provincial Entrepreneurship and Innovation Doctor Program of China, grant number JSSCBS20210926; Industry-University-Research Cooperation Project of Jiangsu Province, grant number BY20230840; Changzhou Sci&Tech Program, grant number CJ20241050.

Institutional Review Board Statement: Not applicable.

Informed Consent Statement: Not applicable.

Data Availability Statement: The data of this study are available from the corresponding author upon request.

Acknowledgments: Thanks to Chen You and Meng Li from Changzhou Institute of Technology for their assistance in other aspects.

Conflicts of Interest: The authors declare no competing interests. Author Zhen Zhong was employed by the company Jiangsu HNP Electric Technology Co., Ltd. There is no conflict of interest between the author and the company Jiangsu HNP Electric Technology Co., Ltd.

References

1. Liu, Q.; Qiao, X.; Jia, Z.; Fu, H.; Gao, H.; Yu, D. Large frequency range and high sensitivity fiber bragg grating accelerometer. *IEEE Sens. J.* **2014**, *14*, 1499–1504. [CrossRef]
2. Jiang, P.; Ma, L.; Hu, Z.; Hu, Y. Low-crosstalk and polarization-independent inline interferometric fiber sensor array based on fiber bragg gratings. *J. Light. Technol.* **2016**, *34*, 4232–4239. [CrossRef]
3. Zhang, M.; Li, Y.; Chen, J.; Song, Y.; Zhang, J.; Wang, M. Event detection method comparison for distributed acoustic sensors using φ-OTDR. *Opt. Fiber Technol.* **2019**, *52*, 101980. [CrossRef]
4. Liu, Z.; Zhang, L.; Wei, H.; Xiao, Z.; Qiu, Z.; Sun, R.; Pang, F.; Wang, T. Underwater acoustic source localization based on phase-sensitive optical time domain reflectometry. *Opt. Exp.* **2021**, *29*, 12880–12892. [CrossRef]
5. Ding, Z.; Zou, N.; Zhang, C.; Chen, Y.; Tong, S.; Wang, F.; Xiong, F.; Zhang, Y.; Zhang, X. Self-optimized vibration localization based on distributed acoustic sensing and existing underground optical cables. *J. Light. Technol.* **2022**, *40*, 844–854. [CrossRef]

6. Liang, J.; Wang, Z.; Lu, B.; Wang, X.; Li, L.; Ye, Q.; Qu, R.; Cai, H. Distributed acoustic sensing for 2D and 3D acoustic source localization. *Opt. Lett.* **2019**, *44*, 1690–1693.
7. Xu, N.; Wang, P.; Wang, Y.; Liu, X.; Bai, Q.; Gao, Y.; Zhang, H.; Jin, B. Crosstalk noise suppressed for multi-frequency φ-OTDR using compressed sensing. *J. Light. Technol.* **2021**, *39*, 7343–7350. [CrossRef]
8. Dong, Y.; Chen, X.; Liu, E.; Fu, C.; Zhang, H.; Lu, Z. Quantitative measurement of dynamic nano-strain based on a phase-sensitive optical time domain reflectometer. *Appl. Opt.* **2016**, *55*, 7810–7815. [CrossRef]
9. Wang, C.; Shang, Y.; Zhao, W.; Liu, X.; Wang, C.; Peng, G. Investigation and comparison of ϕ-OTDR and OTDR-interferometry via phase demodulation. *IEEE Sens. J.* **2018**, *18*, 1501–1505. [CrossRef]
10. Wang, Z.; Pan, Z.; Fang, Z.; Ye, Q.; Lu, B.; Cai, H.; Qu, R. Ultra-broadband phase-sensitive optical time-domain reflectometry with a temporally sequenced multi-frequency source. *Opt. Lett.* **2015**, *40*, 5192–5195. [CrossRef]
11. Pan, Z.; Wang, Z.; Ye, Q.; Cai, H.; Qu, R.; Fang, Z. High sampling rate multi-pulse phase-sensitive OTDR employing frequency division multiplexing. *Proc. SPIE* **2015**, *9157*, 91576X.
12. Wang, Y.; Lu, P.; Mihailov, S.; Bao, X. Ultra-low frequency dynamic strain detection with laser frequency drifting compensation based on a random fiber grating array. *Opt. Lett.* **2021**, *46*, 789–792. [CrossRef] [PubMed]
13. Yang, G.; Fan, X.; Wang, S.; Wang, B.; Liu, Q.; He, Z. Long-range distributed vibration sensing based on phase extraction from phase-sensitive OTDR. *IEEE Photonics J.* **2016**, *8*, 6802412. [CrossRef]
14. Sagues, M.; Piñeiro, E.; Cerri, E.; Minardo, A.; Eyal, A.; Loayssa, A. Two-wavelength phase-sensitive OTDR sensor using perfect periodic correlation codes for measurement range enhancement, noise reduction and fading compensation. *Opt. Exp.* **2021**, *29*, 6021–6035. [CrossRef]
15. Wu, M.; Chen, Y.; Zhu, P.; Chen, W. NLM parameter optimization for φ-OTDR signal. *J. Light. Technol.* **2022**, *40*, 6045–6051. [CrossRef]
16. Zhao, L.; Zhang, X.; Xu, Z. A high-fidelity numerical model of coherent Φ-OTDR. *Measurement* **2024**, *230*, 114526. [CrossRef]
17. Wang, Y.; He, C.; Du, W.; Hu, H.; Bai, Q.; Liu, X.; Jin, B. Interference fading suppression with fault-tolerant Kalman filter in phase-sensitive OTDR. *ISA Trans.* **2024**, *150*, 298–310. [CrossRef]
18. Liang, Y.; Zhang, S.; Zhang, J.; Ye, Z.; Wan, A.; Liu, C.; Sun, J.; Wang, Z. 2D-sensenet: A simultaneous demodulation and denoising network for DAS. *IEEE Trans. Instrum. Meas.* **2024**, *73*, 2511709. [CrossRef]
19. Zhong, Z.; Wang, F.; Zhang, X. Event discrimination using phase correlation in φ-OTDR system based on coherent detection. *IEEE Photonics J.* **2018**, *10*, 7104508. [CrossRef]
20. Zhou, J.; Pan, Z.; Ye, Q.; Cai, H.; Qu, R.; Fang, Z. Characteristics and explanations of interference fading of a φ-OTDR with a multi-frequency source. *J. Light. Technol.* **2013**, *31*, 2947–2954. [CrossRef]
21. Zhong, Z.; Wang, F.; Zong, M.; Zhang, Y.; Zhang, X. Dynamic measurement based on the linear characteristic of phase change in Φ-OTDR. *IEEE Photonics Technol. Lett.* **2019**, *31*, 1191–1194. [CrossRef]
22. Juarez, J.C.; Taylor, H.F. Polarization discrimination in a phase-sensitive optical time-domain reflectometer intrusion-sensor system. *Opt. Lett.* **2005**, *30*, 3284–3286. [CrossRef] [PubMed]